Thermochimica Acta, 203 (1992) 361–372
Elsevier Science Publishers B.V., Amsterdam

Kinetics of crystallization in the soda–lime–silica system. Part 1. $Na_2O \cdot CaO \cdot 2SiO_2$ and $Na_2O \cdot CaO \cdot 3SiO_2$ glasses by DTA

Nobuyoshi Koga [a,1], Jaroslav Šesták [a] and Zdeněk Strnad [b]

[a] *Institute of Physics, Czechoslovak Academy of Sciences, Na Slovance 2, 18040 Prague (Czech and Slovak Federal Republic)*
[b] *Research and Development Institute for Industrial Glass, Glass-Union, Primatorska 51, 180 00 Prague 8 (Czech and Slovak Federal Republic)*

(Received 20 May 1991)

Abstract

DTA curves for the crystallization of the title glasses of various particle size fractions were analysed kinetically using the modified Kissinger method proposed by Matushita and Sakka. The kinetic results were compared with those obtained from microscopic measurements. For the $Na_2O \cdot CaO \cdot 2SiO_2$ glass, it was observed that the kinetic obedience changes from a surface reaction model to a bulk crystallization model with increasing particle size. The values of the apparent activation energy E_{app} corresponded excellently to that obtained microscopically, i.e. 343 kJ mol^{-1}. However, the crystallization of $Na_2O \cdot CaO \cdot 3SiO_2$ glass was regulated by the surface reaction mechanism irrespective of the particle size examined; the values of E_{app} decreased with increasing particle size but no direct correspondence of these values to those determined by the microscopic measurements were found. The complicated behaviour of E_{app} was explained with reference to the role and function of the nucleation at the reaction interface.

INTRODUCTION

Although differential thermal analysis (DTA) has been widely used for the kinetic study of the non-isothermal crystallization of glasses [1,2], it is sometimes difficult to explain the kinetic results obtained by DTA from strictly physical and/or physicochemical points of view [3]. This is apparently due to the complex behaviour of the nucleation and growth processes, and the activation energy obtained from DTA is acknowledged as the

Correspondence to: J. Šesták, Institute of Physics, Czechoslovak Academy of Sciences, Na Slovance 2, 180 40 Prague 8, Czech and Slovak Federal Republic.
Dedicated to Professor Joseph H. Flynn in honour of his 70th birthday.
[1] Permanent address: Chemistry Laboratory, Faculty of School Education, Hiroshima University, Shinonome, Minami-Ku, Hiroshima 734, Japan.

TABLE 1

Activation energies for the nucleation E_N and linear growth E_{LG} determined from microscopic measurements for the isothermal crystallizations of $Na_2O \cdot CaO \cdot xSiO_2$ glasses, bulk sample [5]

x	E_N (kJ mol^{-1})	E_{LG} (kJ mol^{-1})
2	Unmeasurable	343
2.7	285	222
3	No nucleation	213

apparent activation energy E_{app}. In such a situation, it is particularly important to link the kinetic results with those obtained from other physicochemical measurements [4] in order to understand the complex processes more thoroughly and to evaluate the applicability or reliability of DTA.

In the present study, the crystallization of $Na_2O \cdot CaO \cdot 2SiO_2$ (G2) and $Na_2O \cdot CaO \cdot 3SiO_2$ (G3) glasses was investigated because the isothermal crystallization of bulk samples of these glasses has already been investigated systematically by microscopic measurements [5]. The effect of particle size on the kinetics is investigated by DTA. The previous study revealed that $Na_2O \cdot CaO \cdot xSiO_2$ glasses (where $2 < x < 3$) yield $Na_2O \cdot 2CaO \cdot 3SiO_2$ as the crystallization product. The variation in value of x from 2 to 3 leads to a change in the crystallization mechanism from volume crystallization to surface crystallization, accompanied by a decrease in the capability of bulk nucleation. Table 1 summarizes the activation energies obtained from the macroscopic measurements [5]. The significance of the E_{app} values obtained from DTA is analysed on the basis of the above microscopic study. It was hoped that mutual correlation between the properties of the process and E_{app} would be obtained.

EXPERIMENTAL

The glasses were prepared from Reagent Grade SiO_2, $CaCO_3$ and Na_2CO_3. The mixture was decomposed at approx. 900°C for 30 min and then melted at 1450°C in a Pt/5%Rh crucible, stirred from time to time during the melting period of 3 h, and poured into rods approximately 10 mm in diameter. For G2, surface crystallization was observed during the quenching [5]. The crystallized layer was removed by polishing. These glasses were crushed and sieved to various particle size fractions. The samples were stored for one week before DTA measurement to decrease the effect of ageing among the individual DTA runs.

200 mg of each sample was loaded into a platinum crucible 5 mm in diameter and 10 mm in height, and placed in a Linseis DTA system. DTA

traces were recorded at various constant heating rates of 1–20 K min^{-1} under static air. 200 mg of ignited Al_2O_3 was used as reference material.

Kinetic analysis of the DTA data was made using the modified Kissinger equation proposed by Matushita and coworkers [6,7]

$$\ln \frac{\phi^n}{T_p^2} = -\frac{mE_G}{RT_p} + \text{const} \quad (1)$$

where ϕ is the heating rate, T_p the peak temperature and E_G the activation energy for crystal growth. The values of n and m are numerical factors depending on the crystallization mechanism, which result from the assumption of non-exponential nucleation [6–9]. The E_G is thus obtained from sets of data (ϕ, T_p) using pre-assumed values of n and m.

RESULTS AND DISCUSSION

One well-defined exothermic peak corresponding to the crystallization of $Na_2O \cdot 2CaO \cdot 3SiO_2$ was observed for all the sample under the measuring conditions examined.

$Na_2O \cdot CaO \cdot 2SiO_2$ (G2)

It has been reported [5] that for G2 sufficiently dense nuclei are formed both on the surface and in bulk, in the temperature region below that of the crystal growth. Figure 1 shows the DTA crystallization exotherms for G2 of various particle size fractions recorded at a constant ϕ of 10 K min^{-1}. As is usually observed for crystallization regulated by the surface nucleation and growth mechanism, T_p increases with particle size. At the same time, it should be noticed that the peak height does not necessarily

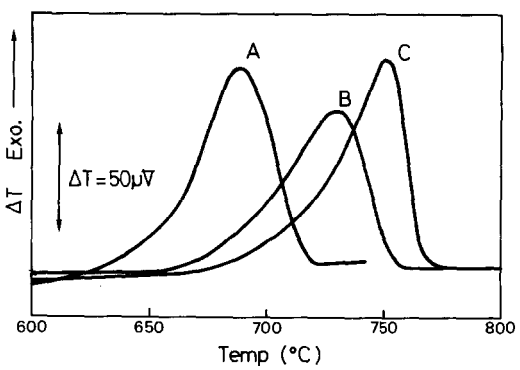

Fig. 1. The DTA exotherms for the non-isothermal crystallization of $Na_2O \cdot CaO \cdot 2SiO_2$ (G2) of various particle size fractions at $\phi = 10$ K min^{-1}: curve A, < 0.1; curve B, 0.2–0.4; and curve C, 0.5–0.7 mm.

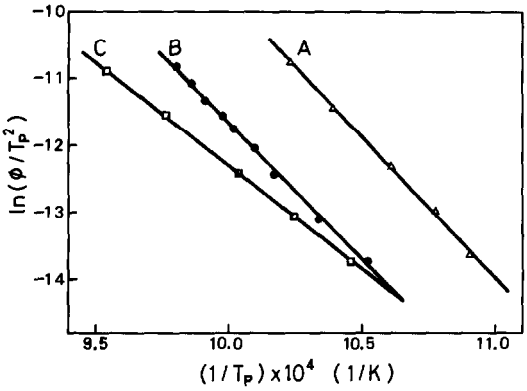

Fig. 2. The Kissinger plots for the non-isothermal crystallization of $Na_2O \cdot CaO \cdot 2SiO_2$ (G2) of various particle size fractions: curve A, < 0.1; curve B, 0.2–0.4; and curve C, 0.5–0.7 mm.

decrease with increasing particle size, in contrast to the case of the surface crystallization mechanism.

The Kissinger plots [10], i.e. $n = m = 1$ in eqn. (1), are shown in Fig. 2. It is clear that the slope of the plot for the sample of particle size 0.5–0.7 mm is apparently different from those of the smaller particle size fractions. Table 2 lists the apparent activation energies for these samples. The value of E_{app} obtained for the smallest particle size fraction (< 0.1 mm) is in good agreement with the activation energy for the linear growth rate, $E_{LG} = 343$ kJ mol^{-1}, determined for the bulk sample by microscopic measurements under isothermal conditions. Accordingly, the crystallization obeys the surface nucleation and one-dimensional growth mechanism and the E_{app} corresponds to the activation energy for crystal growth E_G assumed in eqn. (1). Figure 3 shows the DTA crystallization exotherms for the samples of 0.5–0.7 mm and 1.0–1.4 mm particle size fractions at $\phi = 10$ K min^{-1}. A slight shift in the peak temperature is observed. This means that with these particle size fractions, growth of the bulk nuclei regulates the crystallization. This is supported by the fact that this mechanism is also dominant in the isothermal crystallization of bulk sample [5]. Table 3 shows

TABLE 2

Apparent activation energies E_{app} calculated using the Kissinger method for the non-isothermal crystallization of $Na_2O \cdot CaO \cdot 2SiO_2$ (G2) glasses

Particle size fraction (mm)	Range of T_p (°C)	E_{app} (kJ mol^{-1})	$-\gamma$ [a]
< 0.1	645–703	333 ± 9	0.9995
0.2–0.4	677–737	325 ± 7	0.9995
0.5–0.7	683–775	244 ± 2	0.9999

[a] Correlation coefficient for the linear regression analysis of the Kissinger plot.

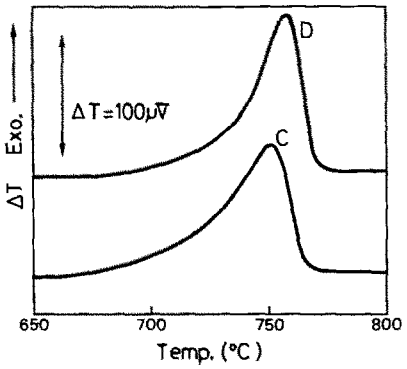

Fig. 3. The DTA exotherms for the non-isothermal crystallization of $Na_2O \cdot CaO \cdot 2SiO_2$ (G2) of particle size fractions: curve C, 0.5–0.7; and curve D, 1.0–1.4 mm at $\phi = 10$ K min^{-1}.

the values of E_{app} calculated from eqn. (1) assuming all possible values of n and m for the 0.5–0.7 mm fraction. When we use the values $n = 4$ and $m = 3$, E_{app} has a value closest to the E_G described above. This indicates that the mechanism of the larger particle size fraction is bulk nucleation and three-dimensional growth, where the number of bulk nuclei is inversely proportional to ϕ.

The change in the crystallization mechanism is likely to result from the variation in the temperature region for the growth of surface nuclei which

TABLE 3

Activation energy for crystal growth E_G calculated according to eqn. (1) for the non-isothermal crystallization of $Na_2O \cdot CaO \cdot 2SiO_2$ (G2) of particle size fraction 0.5–0.7 mm

Reaction geometry	Nucleation behaviour	Rate-controlling step	Growth dimension	n	m	E_G (kJ mol^{-1})	$-\gamma$ [a]
Surface	Zero	Chemical	1	1	1	244 ± 2	0.9999
		Diffusional	1	1/2	1/2	244 ± 2	0.9999
Bulk	Zero	Chemical	1	1	1	244 ± 2	0.9999
			2	2	2	251 ± 2	0.9999
			3	3	3	254 ± 2	0.9999
		Diffusional	1	1/2	1/2	244 ± 2	0.9999
			2	1	1	244 ± 2	0.9999
			3	3/2	3/2	244 ± 2	0.9999
	Constant	Chemical	1	2	1	502 ± 4	0.9999
			2	3	2	381 ± 3	0.9999
			3	4	3	341 ± 3	0.9999
		Diffusional	1	3/2	1/2	733 ± 5	0.9999
			2	2	1	502 ± 4	0.9999
			3	5/2	3/2	408 ± 3	0.9999

[a] Correlation coefficient for the linear regression analysis of the plot according to eqn. (1).

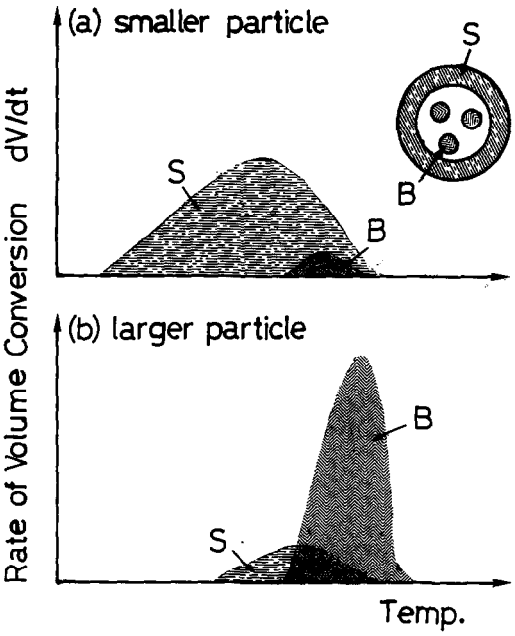

Fig. 4. Schematic representation of the volume fractions crystallized by (S) surface and (B) bulk mechanisms (see text).

depends on the particle size; this is supported by the empirical fact that the DTA exotherm is observed at a lower temperature for the smaller particle sizes when the crystallization is regulated by the surface crystallization mechanism. However, the temperature region for the growth of bulk nuclei is invariant irrespective of particle size, as expected from the constant T_p for the volume crystallization. A possible explanation for the change is represented schematically in Fig. 4. For the smaller particle size, the growth of surface nuclei begins at a temperature significantly lower than that of the bulk nuclei. The one-dimensional growth of surface nuclei leads to the initial generation of a high density of reaction zones. At the sites adjacent to the reaction zones, the bulk nuclei experience enhanced reactivity because of the mechanical strain or stress and self-heating arising from the advance of the reaction zone and they start to growth one-dimensionally. Consequently, the crystallization proceeds according to the advance of the reaction zones from the original surface to the centre of the particle. Even if the sample reaches the temperature of the growth of bulk nuclei before completing the crystallization, the volume fraction crystallized by the volume crystallization mechanism is small, see Fig. 4(a). In contrast to the above, the difference between the temperature regions for the growth of surface and bulk nuclei is smaller for the larger particles, where the volume fraction crystallized by the bulk crystallization mechanism overtakes that crystallized by the advance of the reaction zones,

because of the difference in the reaction frequency of these two mechanisms. Accordingly, the crystallization is expressed predominantly by the three-dimensional growth of bulk nuclei, i.e. Fig. 4(b).

The slight decrease in the E_{app} for the 0.2–0.4 mm sample seems to be due to the combination of the above two mechanisms. It should be acknowledged here that the ratio of volume fractions crystallized by the respective mechanisms changes with ϕ. For the non-isothermal crystallization of $Li_2O \cdot 2SiO_2$ glasses, it was reported [11] that the ratio of volume fraction crystallized by the surface crystallization mechanism increases with ϕ. This implies that, in the case of eqn. (1), the reaction mechanism, i.e. the values of n and m, is a certain mean value among the processes examined at the various ϕ values. The Kissinger plot for the 0.2–0.4 mm sample shows this tendency clearly (see Fig. 2). At the lowest ϕ, i.e. 1.0 K min^{-1}, a slight shift in $1/T_p$ accompanies the change in particle size from 0.2–0.4 to 0.5–0.7 mm. This means that the volume crystallization is already dominant for the 0.2–0.4 mm fraction at this heating rate. In contrast, at the higher heating rates the crystallization of this particle size is still predominantly regulated by the surface crystallization mechanism, supported by the observed trend that the shifts in $1/T_p$ accompanying the change in particle size from 0.2–0.4 to 0.5–0.7 mm increase with ϕ. The heating-rate-dependent increase in the temperature gradient between the surface and bulk seems to be one of the possible reasons for this behaviour.

$Na_2O \cdot CaO \cdot 3SiO_2$ (G3)

It has been reported [5] that for the glasses in this compositional region, no heat treatment can yield homogeneous nucleation and volume crystallization, even with the addition of nucleating agents [12]. This implies that the means of crystallization is by the mechanism of surface nucleation and one-dimensional growth. The DTA crystallization exotherms for G3 of various particle size fractions recorded at a ϕ of 10 K min^{-1} are shown in Fig. 5. With increasing particle size, T_p increases and peak height decreases, as expected for the surface crystallization mechanism. Assuming the above mechanism, the values of $n = m = 1$ can be applied in eqn. (1). Figure 6 shows the Kissinger plots, i.e. $n = m = 1$ in eqn. (1). The slope of the plot decreases slightly with increasing particle size. Table 4 lists the E_{app} values for these samples; they are fairly different from the value of $E_{LG} = 213$ kJ mol^{-1} [5], in contrast to the good agreement obtained for the smallest particle size of G2, in which crystallization is regulated by the same mechanism.

The major difference between the processes that follow the same geometrical mechanism is whether or not the nuclei and/or the nucleus-forming sites exist in the bulk. If the bulk nuclei play an important role in the advance of the reaction interface, then the overall process for G3 consists

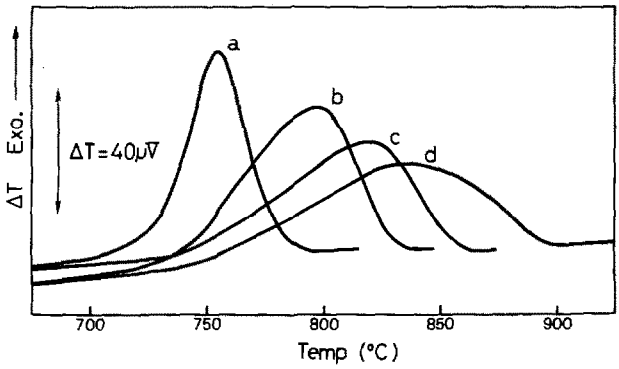

Fig. 5. The DTA exotherms for the non-isothermal crystallization of $Na_2O \cdot CaO \cdot 3SiO_2$ (G3) of various particle size fractions at $\phi = 10$ K min^{-1}: curve a, < 0.1; curve b, 0.2–0.4; curve c, 0.5–0.7; and curve d, 1.0–1.4 mm.

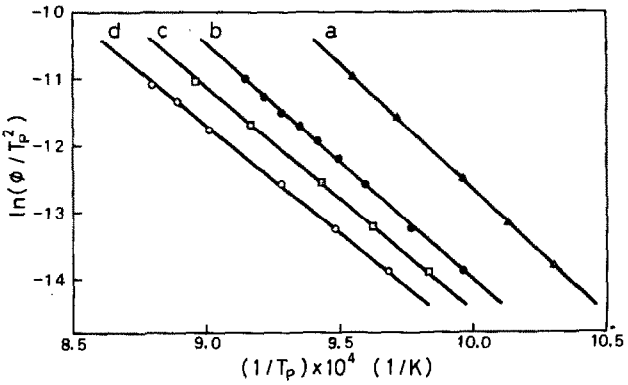

Fig. 6. The Kissinger plots for the non-isothermal crystallization of $Na_2O \cdot CaO \cdot 3SiO_2$ (G3) of various particle size fractions: curve a, < 0.1; curve b, 0.2–0.4; curve c, 0.5–0.7; and curve d, 1.0–1.4 mm.

TABLE 4

Apparent activation energies E_{app} calculated by the Kissinger method for the non-isothermal crystallization of $Na_2O \cdot CaO \cdot 3SiO_2$ (G3) glass

Particle size fraction (mm)	Range of T_p (°C)	E_{app} (kJ mol^{-1})	$-\gamma$ [a]
< 0.1	698–773	303 ± 7	0.9994
0.2–0.4	731–819	282 ± 2	0.9999
0.5–0.7	744–843	256 ± 3	0.9999
1.0–1.4	760–873	253 ± 1	0.9999

[a] Correlation coefficient of the linear regression analysis of the Kissinger plot.

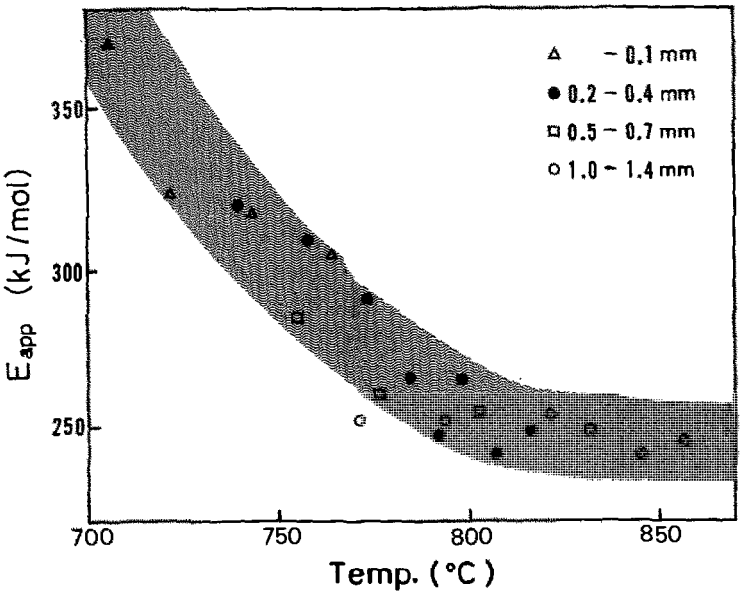

Fig. 7. The plot of E_{app} against temperature for the crystallization of $Na_2O \cdot CaO \cdot 3SiO_2$ (G3).

not only of crystal growth, but also of nucleation at the reaction front. Accordingly, the values of E_{app} do not correspond to E_G, but to the activation energy for the overall process of nucleation and growth, which can be approximated by the equation [1,3,13–16]

$$E_{NG} = \frac{\beta E_N + \lambda E_G}{\beta + \lambda} \tag{2}$$

where E_N is the activation energy for the nucleation, the coefficient β indicates the nucleation law and λ depends on the dimensionality and rate-controlling step of the growth. The value of β is zero, i.e. zero-rate nucleation for G2 of smaller particle sizes and not equal to zero for G3.

It should be noted that the decrease in E_{app} with increasing particle size is accompanied by a shift in the range of T_p to the higher temperature region (see Table 4). Figure 7 shows the temperature dependence of E_{app} obtained from the T_p of the nearest two ϕ values for respective particle size fractions using the Kissinger equation. It is clear that E_{app} depends not only on the particle size, but also on the temperature. In the temperature region below 800°C, the E_{app} decreases with increasing temperature. This is probably explained by the change in the nucleation behaviour, depending on particle size and temperature, which is due to the change in curvature of the reaction front, the temperature-dependent structural relaxation, the role of diffusion processes, etc. Unfortunately, at present there is no effective kinetic description for such a complicated process [17]. However,

above 800°C, the E_{app} shows a constant value of around 250 kJ mol^{-1}, irrespective of particle size. This temperature region corresponds to that of the previous isothermal study [5].

It is interesting here to review the isothermal crystallization of $Na_2O \cdot CaO \cdot 2.7SiO_2$ (G2.7) [5]. For this glass the same linear growth rate was observed for both the surface and bulk crystallization, with $E_{LG} = 222$ kJ mol^{-1}. Judging from the good agreement in the values of E_{LG} for G2.7 and G3, E_{LG} is also likely to correspond to E_G in the case of G3. By assuming constant rate nucleation, i.e. $\beta = 1$, an E_N value of 289 kJ mol^{-1} for the crystallization of G3 at temperatures above 800°C can be derived from eqn. (2). This value corresponds closely to the E_N value for the bulk nucleation of G2.7 (285 kJ mol^{-1}) which is the boundary composition for the bulk nucleation.

Correction of E_{app}

In spite of the complex kinetic process of the crystallization of glasses [18], the kinetic model function applied is usually the oversimplified mathematical description based on the movement of the reaction interface and its geometry [1,16,19]. An analysis of the J–M–A–Y–K equation shows that the E_{app} obtained using this equation is the sum of the partial energies of nucleation (E_N) and growth (E_G), where the movement of the reaction interface is controlled by either chemical reaction at the reaction front or diffusion of constituent atoms, as shown in eqn. (2) [13]. When the nucleation temperature region is fully separated from that of growth, the values of β and E_N in eqn. (2) can be considered to be zero. Then, E_{app} corresponds directly to the activation energy for the rate-controlling step of the reaction interface movement. Such a relatively simple process can be produced by heating the sample in the region of the nucleation temperature [7,20–23] or by adding the nucleating agents [2].

Although the expression in eqn. (2) cannot strictly be applied to crystallization at a linearly increasing temperature [15], we sometimes encounter good agreement between the values of E_G corrected according to eqn. (2) and the activation energy determined by other physicochemical techniques. As can be seen from the crystallization process of G2 fractions of larger particle size, it is sometimes necessary to take into account the change in the number of nuclei which depends on ϕ [6–9,20–23]. When the number of nuclei is inversely proportional to ϕ, the value of E_{app} obtained by the Kissinger method can be corrected according to eqn. (2) by substituting $E_N = 0$ and $\beta = 1$. Because in the Matushita–Sakka equation, $n = \beta + \lambda$ and $m = \lambda$ are assumed, eqn. (1) which has been used successfully for similar processes, can be regarded as an example of the correction of E_{app} using eqn. (2) [24].

Another example of the correction is for the process where only surface nucleation is dominant, followed by growth, as in the case of G3. In this case, E_{app} sometimes changes with particle size [25]. By assuming that the change in the number of surface nuclei depends on the surface curvature, Strnad and Šesták established the correspondence between E_{app} from DTA and E_{LG} from optical measurements by the correction using $E_N = 0$, $\beta = 1$ and $\lambda = 3$ in eqn. (2) [4]. In the present study, it was observed for the similar process that the E_{app} changes depend not only on the particle size, but also on the growth temperature. For such a process with a particularly slow surface reaction, the identification of an activation energy requires perhaps greater knowledge of the specialized conditions prevailing at the reaction interface than is often available, or assumptions that cannot be demonstrated [26]. As an attempt to describe such a complex kinetic process, the concept of the role and function of the nucleation at the reaction front [27–29] was introduced to interpret the variation in E_{app}. For the temperature region in which E_{app} does not change, a constant rate of nucleation at the reaction front, $\beta = 1$, and one-dimensional growth of these nuclei, $\lambda = 1$, were assumed. The values of E_N and E_G obtained by the correction using eqn. (2) corresponded to those determined microscopically. At the same time, the change in E_{app} with the temperature can be interpreted as one of the different aspects of the so-called kinetic compensation effect (KCE) [30–32]. The KCE results from the complex interactions of more than one cause [33] including the discrepancy between the theoretical model and the real kinetic process [34]. In this sense, a quantitative explanation for the establishment of KCE relaxed directly with a certain physicochemical factor seems to be difficult [35].

REFERENCES

1 J. Šesták, Thermophysical Properties of Solids, Elsevier, Amsterdam, 1984.
2 Z. Strnad, Glass-Ceramic Materials, Elsevier, Amsterdam, 1986.
3 J. Šesták, Thermochim. Acta, 98 (1986) 339.
4 Z. Strnad and J. Šesták, in J. Woods (Ed.), Reactions of Solids, Plenum Press, New York, 1977, p. 553.
5 Z. Strnad and R.W. Douglas, Phys. Chem. Glasses, 14 (1973) 33.
6 K. Matushita and S. Sakka, J. Non-Cryst. Solids, 38,39 (1980) 741.
7 K. Matushita, T. Komatu and R. Yokota, J. Mater. Sci., 19 (1984) 291.
8 K. Matushita and S. Sakka, Thermochim. Acta, 33 (1979) 351; Phys. Chem. Glasses, 20 (1979) 81.
9 K. Matushita, K. Miura and T. Komatsu, Thermochim. Acta, 88 (1985) 283; Yogyo Kyokai Shi, 94 (1986) 941.
10 H.E. Kissinger, Anal. Chem., 29 (1957) 1702.
11 K. Matushita, S. Sakka and Y. Matsui, J. Mater. Sci., 10 (1975) 961.
12 Z. Strnad, Glass-Ceramic Materials, Elsevier, Amsterdam, 1986, p. 72.
13 J. Šesták, Phys. Chem. Glasses, 15 (1974) 137.
14 S. Ranganathan and M.V. Heimendahl, J. Mater. Sci., 16 (1981) 2401; 2405.

15 T. Kemeny and J. Šesták, Thermochim. Acta, 110 (1987) 113.
16 J. Šesták, in Z. Chvoj, J. Šesták and A. Triska (Eds.), Kinetic Phase Diagrams, Elsevier, Amsterdam, 1991, Chapter 6, p. 211.
17 N.P. Bansal and R.H. Doremus, J. Therm. Anal., 29 (1984) 115.
18 J. Šesták and V. Šestáková, in Thermal Analysis, (Proc. 5th ICTA), Kyoto, Heyden, London, 1978, p. 111.
19 S.F. Hulbert, J. Br. Ceram. Soc., 1 (1970) 11.
20 A. Marotta, S. Saielli, F. Branda and A. Buri, Thermochim. Acta, 46 (1981) 123; J. Mater. Sci., 16 (1981) 341.
21 C.R. Ray and D.E. Day, J. Am. Ceram. Soc., 73 (1990) 439.
22 X.J. Xu, D.E. Day and C.R. Ray, J. Therm. Anal., in press.
23 R.K. Kadiyala and C.A. Angell, Colloids and Surfaces, 11 (1984) 341.
24 T. Ozawa, Bull. Chem. Soc. Jpn., 57 (1984) 639, 952; Thermochim. Acta, 135 (1988) 85.
25 J. Muller, J. Therm. Anal., 35 (1989) 823.
26 M.E. Brown, D. Dollimore and A.K. Galwey, Reactions in the Solid State, Elsevier, Amsterdam, 1980, p. 95.
27 A.K. Galwey, K. Spinicci and G.G.T. Guarini, Proc. R. Soc. London Ser. A, 378 (1981) 477.
28 H. Yoshioka, K. Amita and G. Hashizume, Netsu Sokutei, 11 (1984) 115 (in Japanese).
29 Y. Masuda, K. Iwata, R. Ito and Y. Ito, J. Phys. Chem., 91 (1987) 6543.
30 N. Koga and H. Tanaka, J. Therm. Anal., 37 (1991) 347.
31 N. Koga and J. Šesták, J. Therm. Anal., 37 (1991) 1103.
32 N. Koga and J. Šesták, Thermochim. Acta, 182 (1991) 201.
33 N. Koga, Ph.D. Thesis, Technical University of Pardubice, Czechoslovakia, 1991.
34 N. Koga, J. Šesták and J. Málek, Thermochim. Acta, 188 (1991) 333.
35 H. Tanaka, N. Koga and J. Šesták, Tanaka, Thermochim. Acta, 203 (1992) 203.